FRET BIOSENSOR: potential *in vivo* applications for pharmacodynamics and drug discovery

Bei Li
Institute of Neuropathology, USZ
Technical Journal Club

Outline

1. Introduction of FRET biosensor
2. Application Paper-1
3. Application Paper-2
4. Summary & Future perspectives

What is FRET ?

Förster (or fluorescence) **R**esonance **E**nergy **T**ransfer:

"A radiationless energy transfer process from a donor fluorophore to an acceptor fluorophore placed in close proximity to the donor."

Nat Biotechnol. 2003 Nov;21(11):1387-95

FRET efficiency, E is very sensitive to the distance between fluorophores.

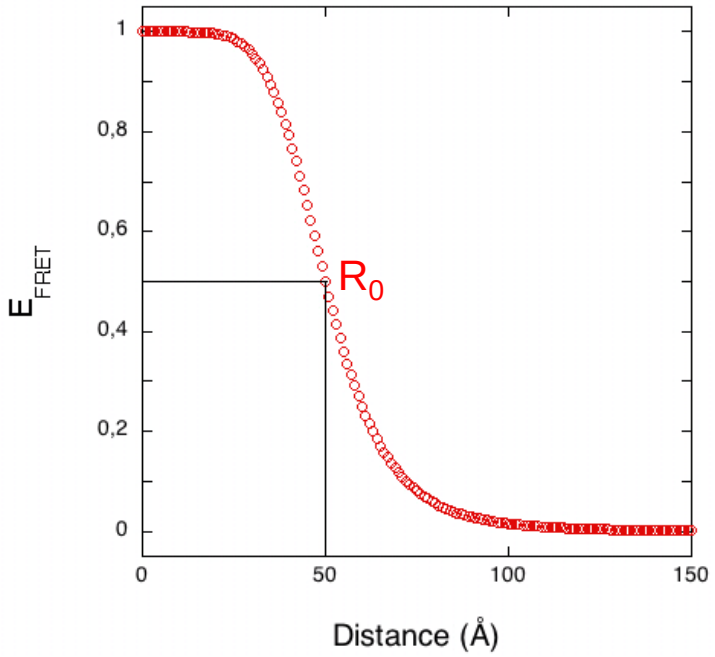

$$E = \frac{(R_0/r)^6}{1+(R_0/r)^6}\,;\, R_0^6 = c_0\kappa^2 J n^{-4} Q_0$$

- **r** is the distance between donor and acceptor
- **R_0** is the Förster distance where the FRET efficiency **E** becomes 0.5
- **Q_0** is the quantum yield of the donor

e.g. CFP/YFP FRET pair, no FRET at r > 11 nm (100 Å)

In practical terms, FRET efficiency is dependent on r, k^2, J

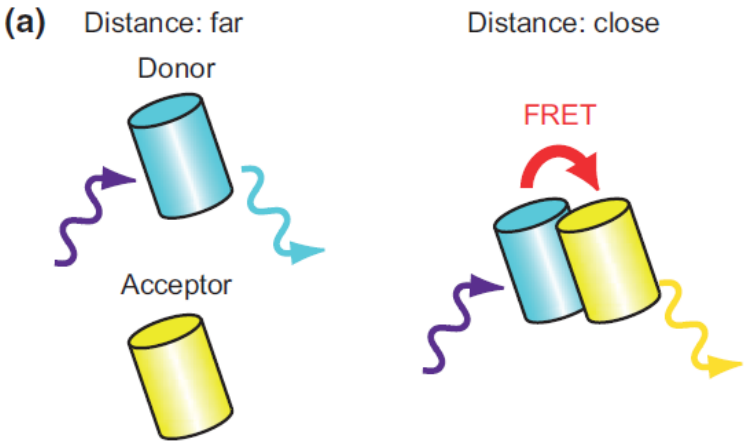

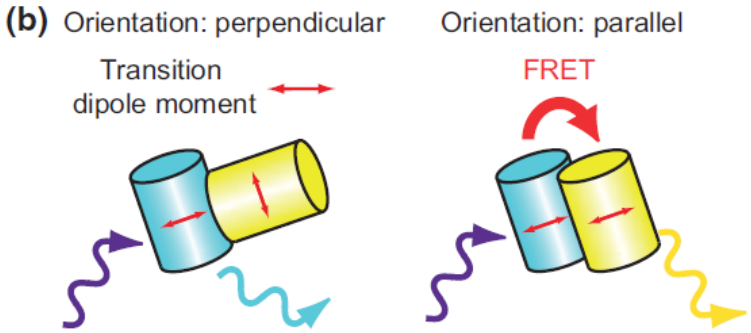

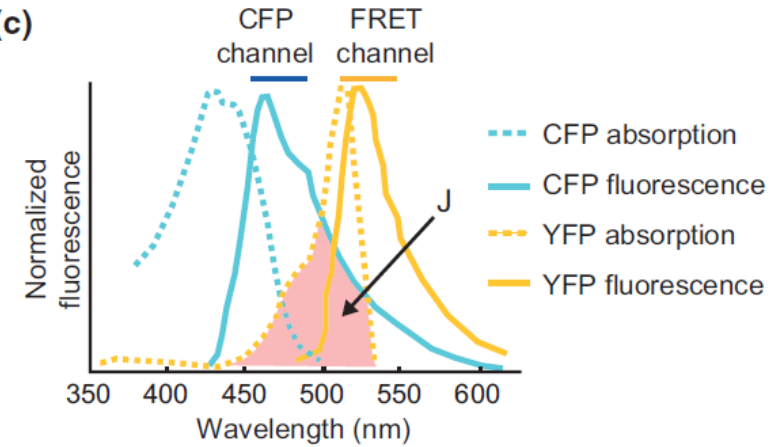

a) **r**: the distance between donor and acceptor

b) **k^2**: a factor determined by the relative orientation of transition moments of the donor and acceptor

c) **J**: the overlap of the donor emission and acceptor excitation spectra

Dev Growth Differ. 2013 May;55(4):515-22.

What is FRET biosensor ?

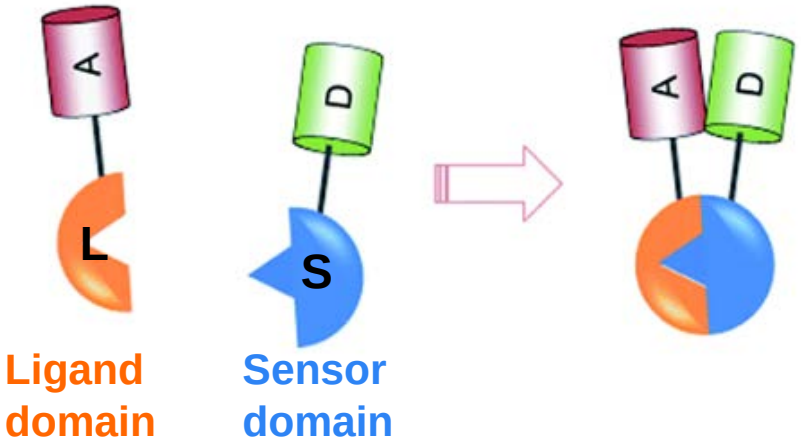

A FRET biosensor usually consists of a donor, a sensor domain, a ligand domain and an acceptor,

- The sensor domain senses the alteration in environmental signal, which induces conformational change of the sensor domain.
- The ligand domain recognizes the conformational change of the sensor domain, leading to the change in FRET efficiency.

Two types of FRET biosensors: Intermolecular and Intramolecular

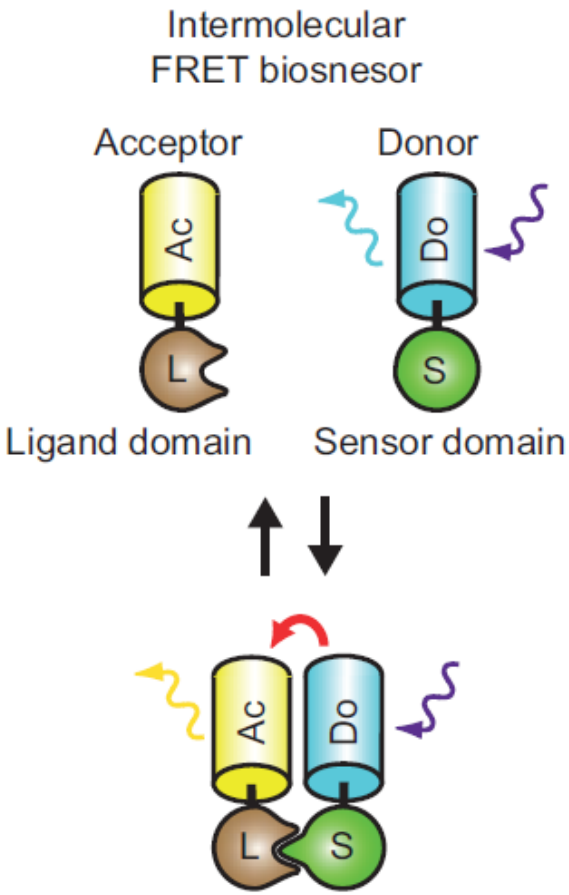

1) Intermolecular

- It consists of a protein fused with a donor and another protein fused with an acceptor.
- When the two proteins associate with each other, FRET takes place between the fluorescent proteins.

Limitations for *in vivo* application:

– It is difficult to introduce equal amounts of donor- and acceptor-fusion proteins into a single cell.

– The donor- and acceptor-fusion proteins usually have different subcellular distribution (unevenness).

Dev Growth Differ. 2013 May;55(4):515-22.

Two types of FRET biosensors: Intermolecular and Intramolecular

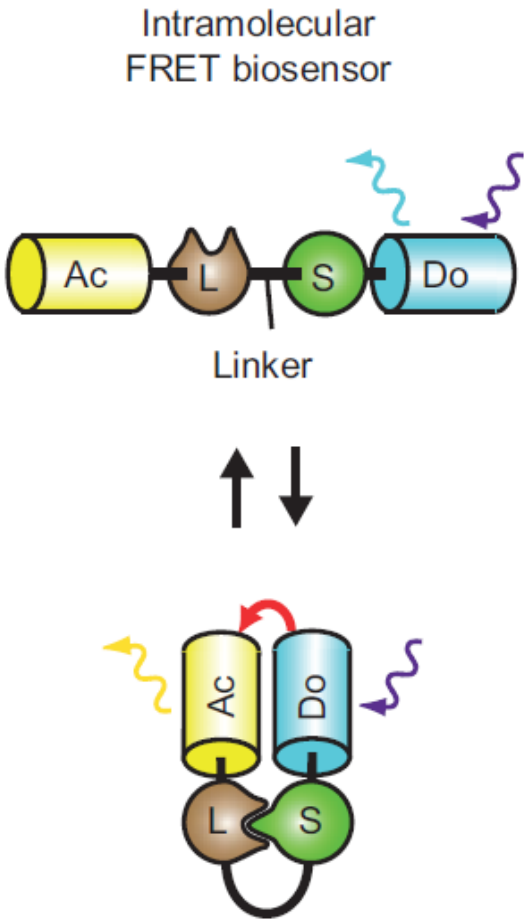

2) Intramolecular

- It consists of a pair of fluorescent proteins, sensor and ligand domains connected by a linker.
- Upon stimulation, the conformation of the sensor region is changed so that it binds to the ligand region.

The use of intramolecular FRET biosensors has been steadily increasing.

Dev Growth Differ. 2013 May;55(4):515-22.

Five themes of intramolecular FRET biosensors

According to the potential *in vivo* application for research and drug discovery, the intramolecular FRET biosensors have been broadly classed into five themes:

(1) Cleavage-based

(2) Substrate-based

(3) Binding domain-based

(4) Tag-based

(5) Sensitivity-based

(1) Cleavage-based

- The biosensor itself is irreversibly cleaved by the protein in question for which loss of FRET upon cleavage of the biosensor can be used to measure activity.

- For example, the caspase 3 biosensor: When caspase 3 is active, the single-peptide sensor DEVD (caspase cleavage sequence) is cleaved, increasing the distance between CFP and eYFP, resulting in increased CFP fluorescence and decreased FRET.

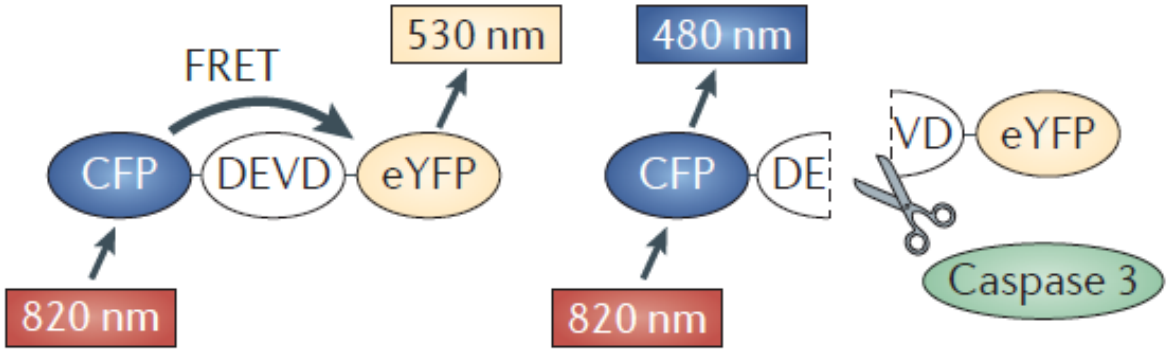

Nat Rev Cancer. 2014 Jun;14(6):406-18.

(1) Cleavage-based

Role	Target(s)	Pathway(s)
Apoptosis	Caspase 3	• Caspase-dependent cell death • Inflammatory response
	Caspase 8	Apoptosis
Autophagy	ATG4A or ATG4B	Autophagosome biogenesis
ECM remodelling	MT1MMP	• Cell migration or invasion • Cell adhesion

- They can only read out biological processes for which reversibility of the biosensor is NOT required.

Nat Rev Cancer. 2014 May;14(5):314-28.

(2) Substrate-based

- The biosensors are tagged proteins that are phosphorylated by the target in question.

- For example, the Src biosensor contains an ECFP, a flexible linker connecting SH2 (Src Homology 2) domain and a substrate sequence, and a YPet. The substrate can be specifically phosphorylated by active Src kinase (proto-oncogene tyrosine-protein kinase), subsequently binding to the intramolecular SH2 domain, and resulting in increased ECFP and decreased FRET.

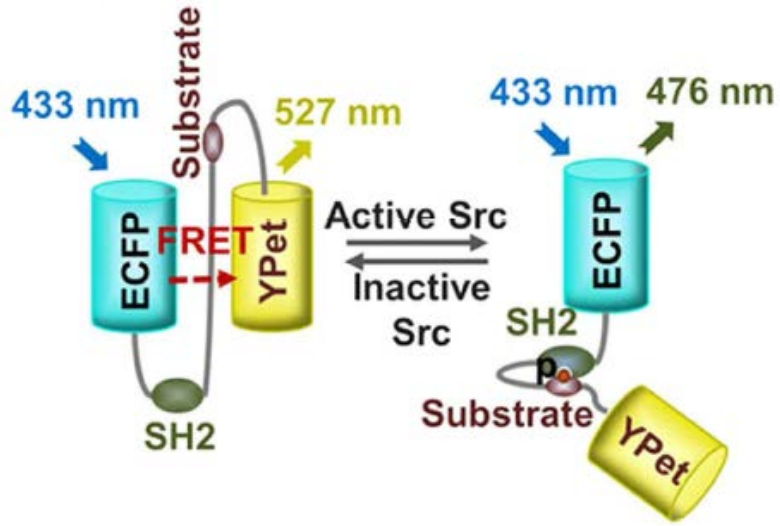

Sci Rep. 2015 Aug 11;5:12963.

(2) Substrate-based

Role	Target(s)	Pathway(s)
Cell division	CDK or cyclins	• Cell cycle progression • Proliferation
	PLK1	• DNA damage response • Cell cycle progression
Signal transduction	AKT (PKB)	• Survival • Metabolism • Apoptosis
	ERK	• Extracellular signal transduction • Proliferation • Differentiation
Cell–cell adhesion	FAK	• Cell adhesion • Proliferation • Integrin-mediated signalling cascades
	SRC	• Differentiation • Migration • Proliferation or survival

- They can be de-phosphorylated, giving the reversibility that is required for dynamic drug studies, monitoring drug turnover and clearance.
- The method can demonstrate spatiotemporal drug activity (e.g. revealed that SRC activity is increased at the invasive border of the tumour), which could not have been discovered using conventional techniques such as the measurement of plasma drug concentrations.

Nat Rev Cancer. 2014 May;14(5):314-28.

(3) Binding domain-based

- The biosensors are reversibly associated with a linked binding domain, in a GTP-bound form.

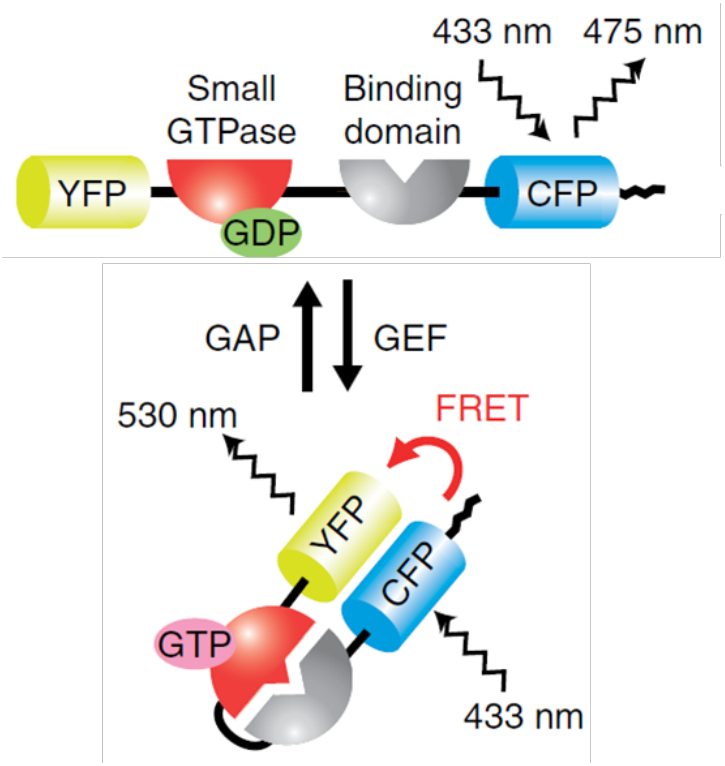

- The binding domain is a part of effector protein of the small GTPase.
- When the GTPase is bound to GDP, no FRET occurs. When the GTPase is bound to GTP, its intramolecular association with the binding domain brings acceptor (YFP) into a close proximity of donor (CFP).

Nat Protoc. 2009;4(11):1623-31.

(3) Binding domain-based

Role	Target(s)	Pathway(s)
Motility	RHOA, RAC and CDC42	• Actin cytoskeletal remodelling • Cell–cell junction dynamics • Cell motility • ROS production • Proliferation
	RAS	• Tumour initiation • Proliferation • Differentiation

- To maintain physiological relevance, strict control must be maintained for expression levels of biosensors to avoid the sequestration or alteration of upstream and/or downstream signaling activity within cells.

Nat Rev Cancer. 2014 May;14(5):314-28.

(4) Tag-based

- These biosensors are dependent on a conformational change of a protein that has two domains tagged with a FRET pair.

- For example, the glucose biosensor: the glucose/galactose binding protein MglB (D-galactose-binding periplasmic protein, from E. coli), consisting of two lobes and a hinge region, is coupled terminally with a CFP and a YFP. The glucose bound state leads to increased FRET.

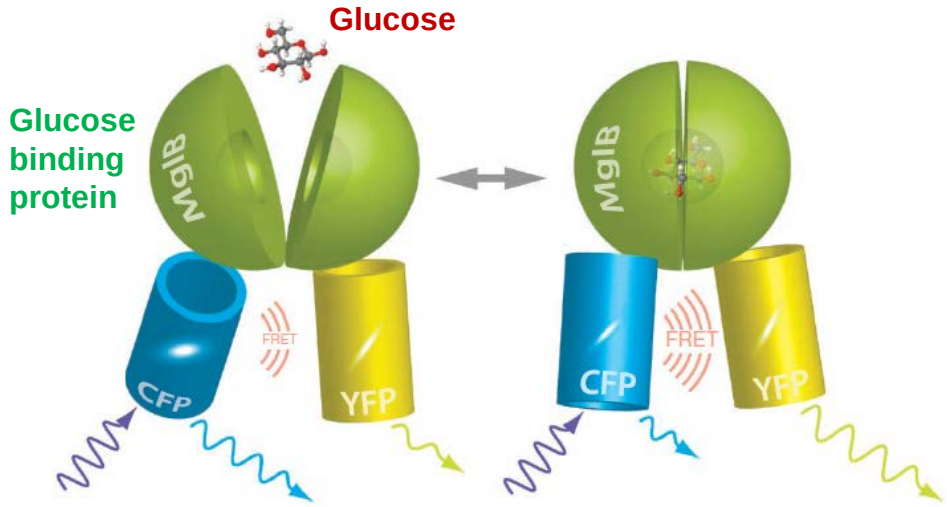

Nat Protoc. 2011 Oct 27;6(11):1818-33.

(4) Tag-based

Role	Target(s)	Pathway(s)
Metabolism	ATP	Intracellular energy transport
	Glutamate	Protein metabolism
	Glucose	Respiration

- These biosensors provide spatiotemporal quantifications of metabolic changes.

Nat Rev Cancer. 2014 May;14(5):314-28.

(5) Sensitivity-based

- These biosensors provide a dynamic method for detecting levels of intracellular components, such as oxygen and pH.

- For example, the oxygen biosensor FluBO for detecting intracellular oxygen uses an oxygen-insensitive donor fluorescent protein FbFP (hypoxia-tolerant flavin-binding fluorescent protein) that is intramolecularly linked to an oxygen-sensitive acceptor fluorescent protein, and thus FRET only occurs in the presence of oxygen.

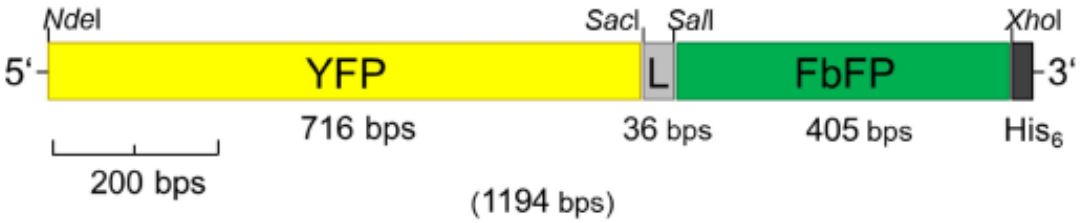

BMC Biol. 2012; 10: 28.
Nat Rev Cancer. 2014 May;14(5):314-28.

(5) Sensitivity-based

Role	Target(s)	Pathway(s)
Hypoxia	O_2	Energy homeostasis
Stress	pH	• Cytosolic homeostasis • Enzymatic processes • Cell cycle progression • Cell proliferation • Apoptosis induction

- Blood flow, oxygen delivery and consumption, and hypoxia, are important aspects of *in vivo* cancer biology. The dual imaging of these factors that may influence tumour behaviour with altered drug-target signalling, could potentially be co-monitored using these distinct but interdependent types of FRET biosensor readouts.

Nat Rev Cancer. 2014 May;14(5):314-28.

Paper-1

CELL STRUCTURE AND FUNCTION 37: 65–73 (2012)

Live Imaging of Protein Kinase Activities in Transgenic Mice Expressing FRET Biosensors

Yuji Kamioka[1,2†], Kenta Sumiyama[3†], Rei Mizuno[1,4], Yoshiharu Sakai[4], Eishu Hirata[5], Etsuko Kiyokawa[1], and Michiyuki Matsuda[1,5*]

[1]*Department of Pathology and Biology of Diseases, Graduate School of Medicine, Kyoto University, Kyoto*

- The application has been mostly limited to cultured cells that express the FRET biosensor constructs, due to particular difficulties in the development of transgenic mice with FRET biosensors.
- This paper describes the efficient generation of transgenic mouse lines expressing heritable and functional biosensors for protein kinase.

The substrate-based FRET biosensor for PKA and ERK

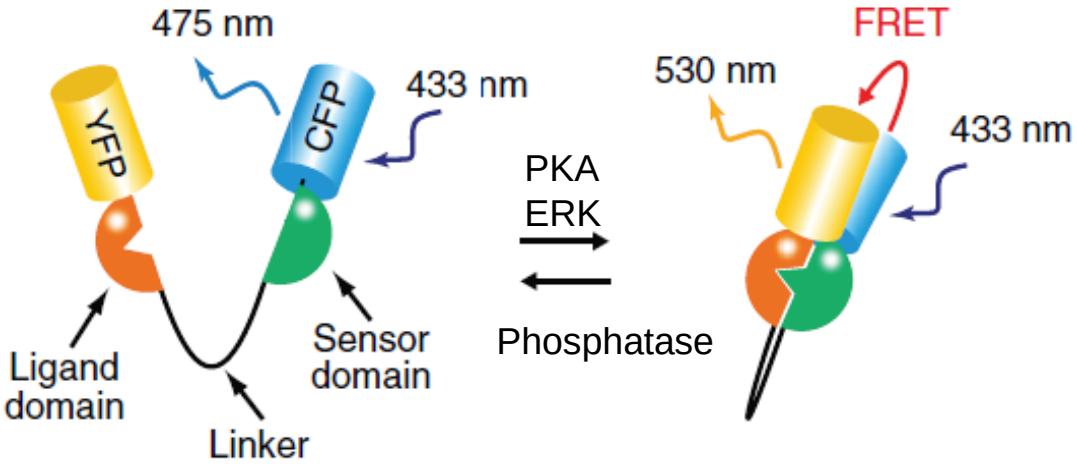

- PKA (Protein kinase A) is a cAMP-dependent protein kinase. PKA phosphorylates substrates in both the cytoplasm and nucleus.
- ERKs (Extracellular signal-regulated kinases) are classical MAP kinases. Phosphorylation of ERKs leads to the activation of their kinase activity.

Phosphorylation of the biosensor by each kinase induces conformational change and increases in FRET.

An optimized backbone of FRET biosensor

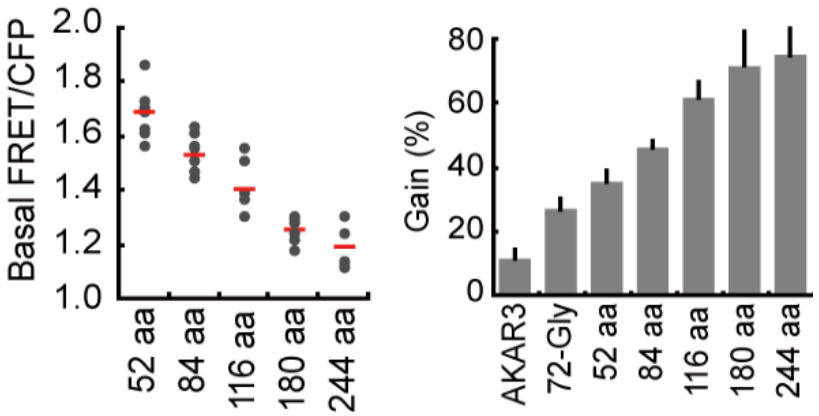

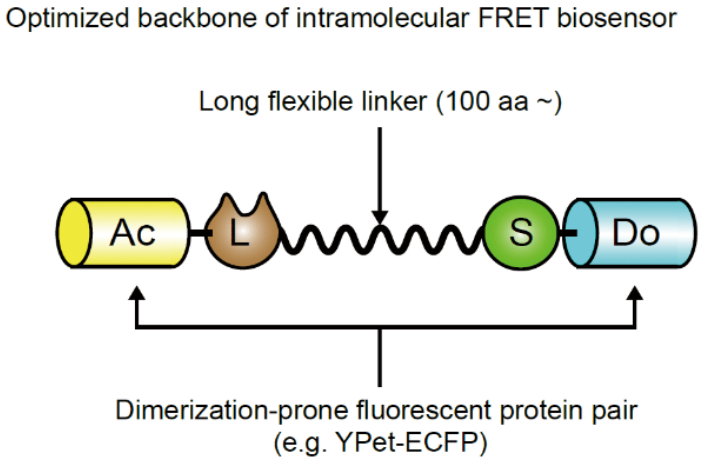

- To exclude the “orientation-dependent” FRET and to render the biosensors completely “distance-dependent”, they optimized a pair of fluorescent proteins for distance-dependent biosensors, and then developed a long, flexible linker ranging from 116 to 244 amino acids in length, which reduced the basal FRET signal and thereby increased the gain of the FRET biosensors.

Mol Biol Cell. 2011 Dec;22(23):4647-56.

The structure of PKA and ERK FRET biosensor

PKA biosensor:

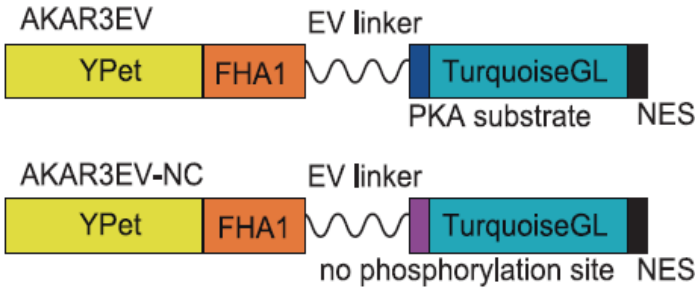

ERK biosensor:

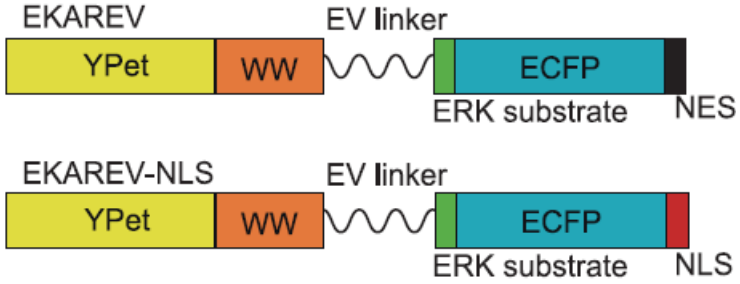

The structure of FRET biosensor:

- Donor: TurquoiseGL, or ECFP
- Acceptor: Ypet
- Phosphate binding domain: FHA1 (forkhead-associated domain), or WW (rsp5 domain)
- Senser domain: PKA or ERK substrate
- EV linker: a 116 amino-acid flexible linker
- NES (nuclear exclusion signal)
- NLS (nuclear localization signal)

Expressing FRET biosensor by Tol2 transposon system

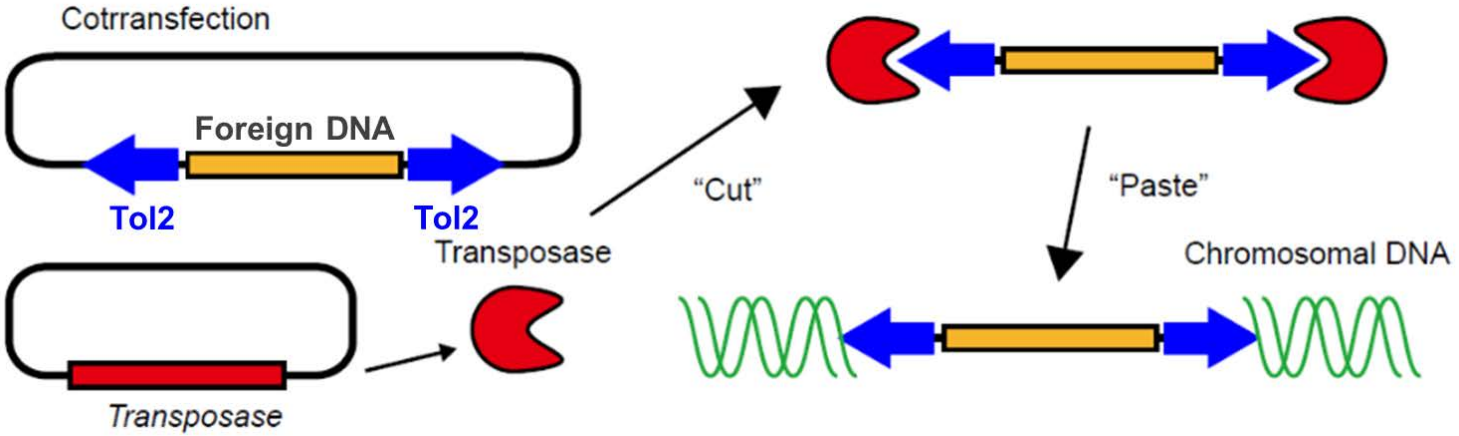

- The medaka fish Tol2 element is an autonomous transposon that encodes a fully functional transposase.
- The transposase protein can catalyze transposition of a transposon construct that has 200 and 150 bp of DNA from the left and right ends. These sequences contain essential terminal inverted repeats (TIRs) and subterminal regions that are sufficient and required for transposition.
- DNA inserts of fairly large sizes (as large as 11 kb) can be cloned between these sequences without reducing transpositional activity.

Tol2-mediated cytoplasmic injection

The Tol2 transposon system has been shown to be active from fish to mammals:

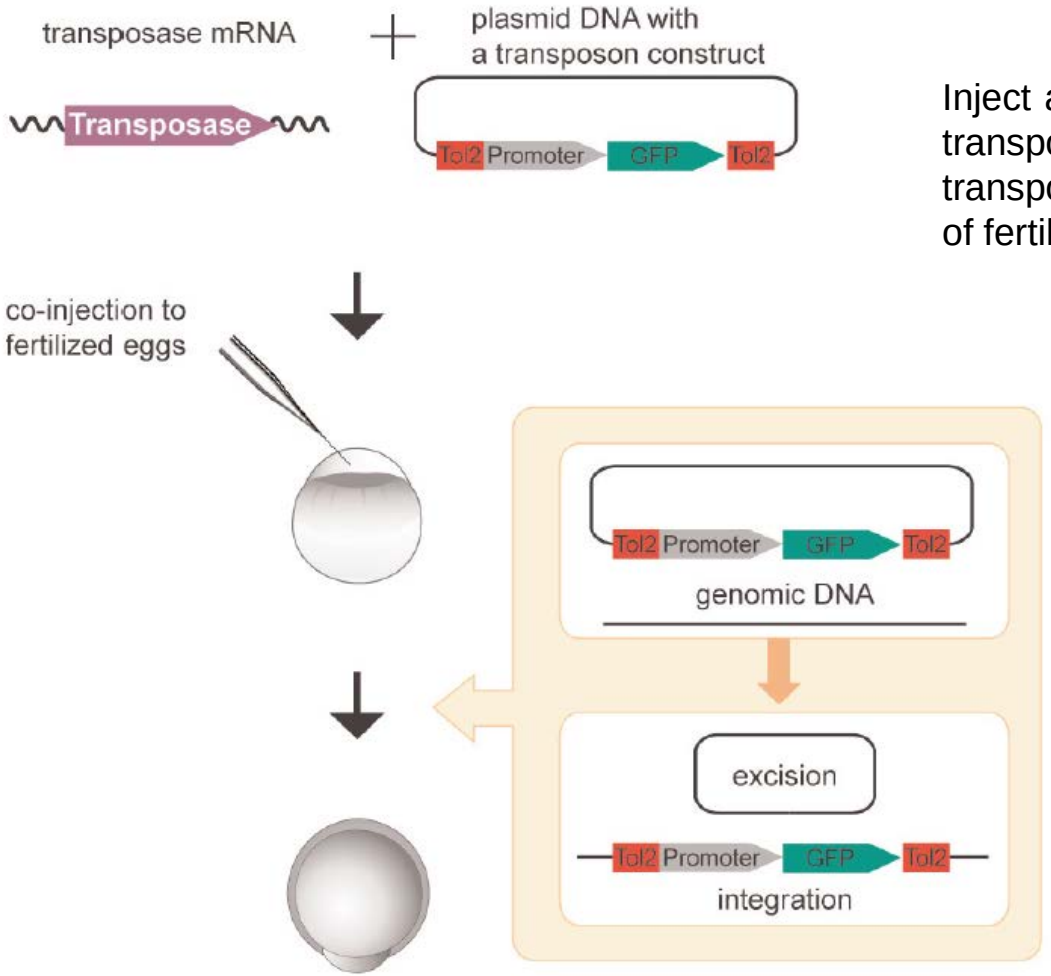

Inject a foreign DNA cloned in a Tol2-transposon vector together with the transposase mRNA into the cytoplasm of fertilized eggs.

The foreign DNA was transposed from the plasmid to the genome and transmitted to the next generation very efficiently.

Genomics. 2010 May;95(5):306-11.

Transgenic mice expresscing FRET biosensers

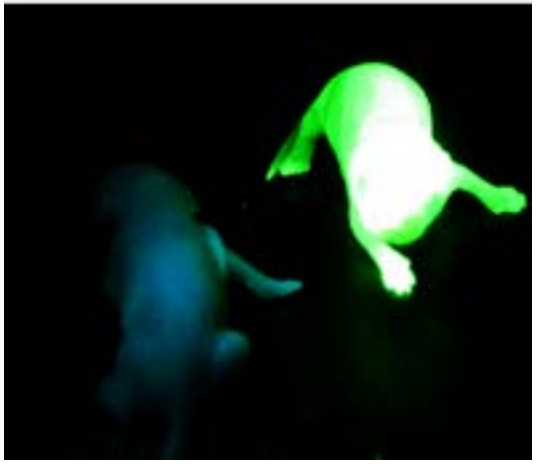

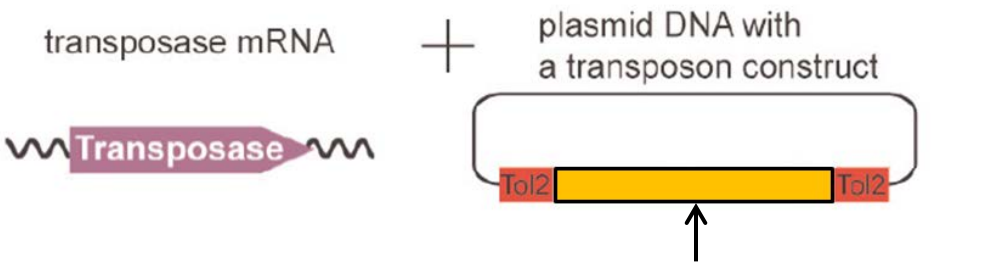

CAG-promoter driven expression cassettes of FRET biosensors were insterted into the pT2A vector.

- The pT2A-derived expression plasmid and Tol2 mRNA were co-injected into mouse oocytes.
- With CAG promoter, the FRET mice are bright enough to be screened under UV light at birth.
- The Mouse viability ranged from 23% to 47%. The integration rate ranged from 5% to 41%.
- Until the sixth generation of the transgenic mouse lines, the FRET biosensors were functional without any detectable change in the expression level.

PKA activation in laser-ablated epidermis

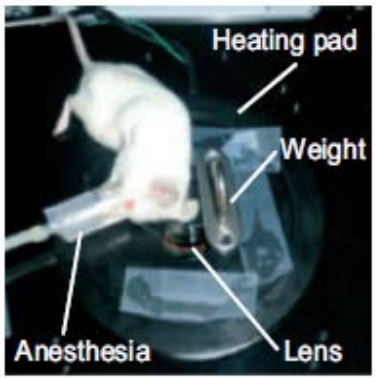

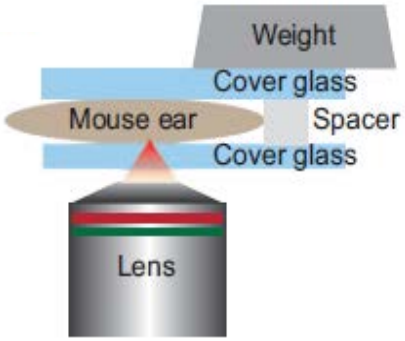

Two-photon excitation microscopy (TPEM)

a region of interest

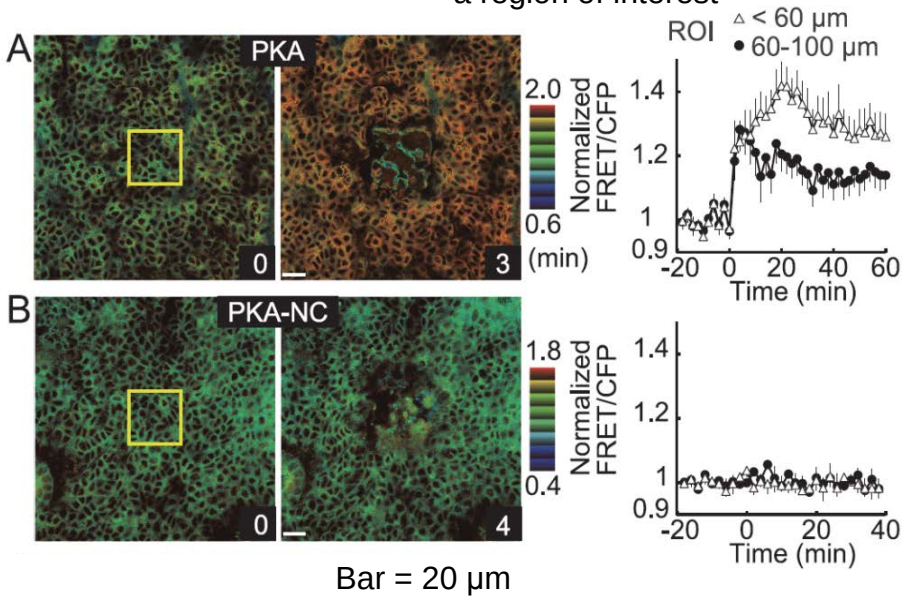

Bar = 20 μm

Upon localized laser ablation of the ear epithelium, PKA was rapidly and diffusely activated in the squamous epithelium, as monitored by the increase in FRET/CFP ratio.

- In squamous cells adjacent to the injured region (<60 μm), PKA was activated immediately (<1 min), followed by a longer period of sustained activation.
- Meanwhile, in cells 60 to 100 μm from the lesion, a gradual decrease in PKA activity followed the initial response.

suggested that the immediate response in PKA was caused by heat, and that the sustained activation was the result of chemical mediators.

ERK activation in laser-ablated epidermis

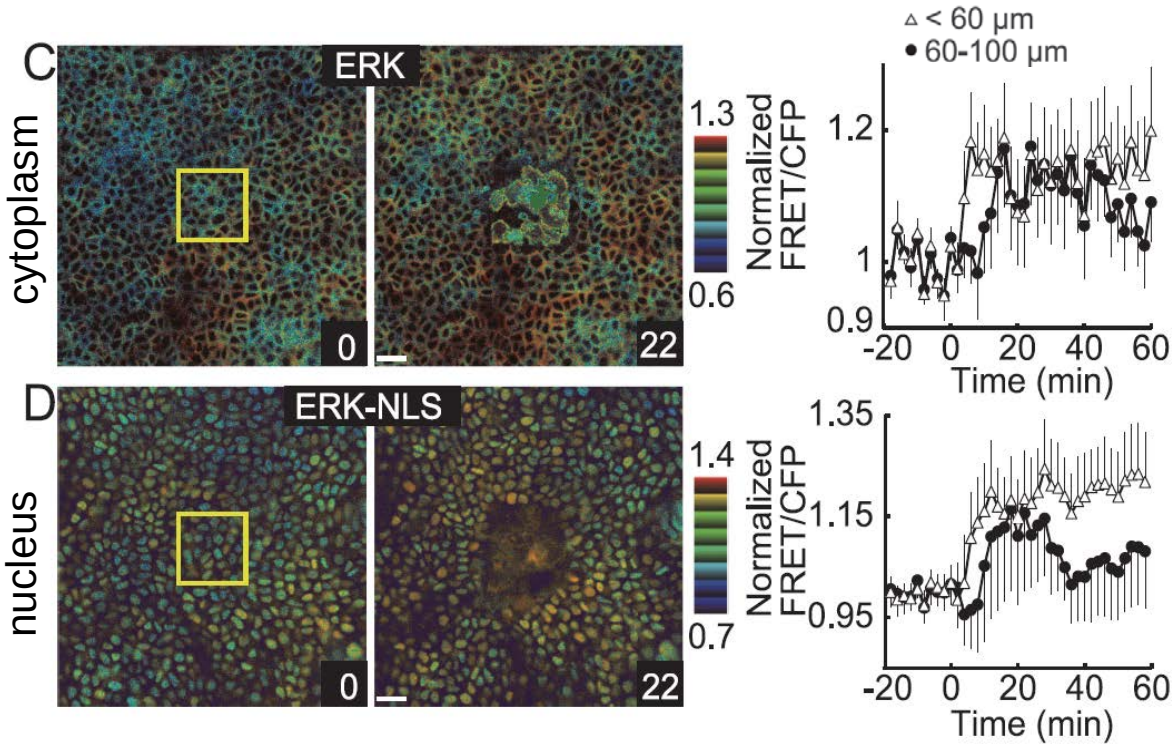

- In basal layer cells adjacent to laser-ablated lesions, ERK was rapidly activated, followed by a gradual increase in activity, which peaked at 10 min.
- The initiation of activation was delayed in cells adjacent to the lesion in a distance-dependent manner.

Real-time visualization of pharmacodynamics in granulocytes

The FRET image of ear dermis in a transgenic mouse, 4h after treatment with 10% arachidonic acid.

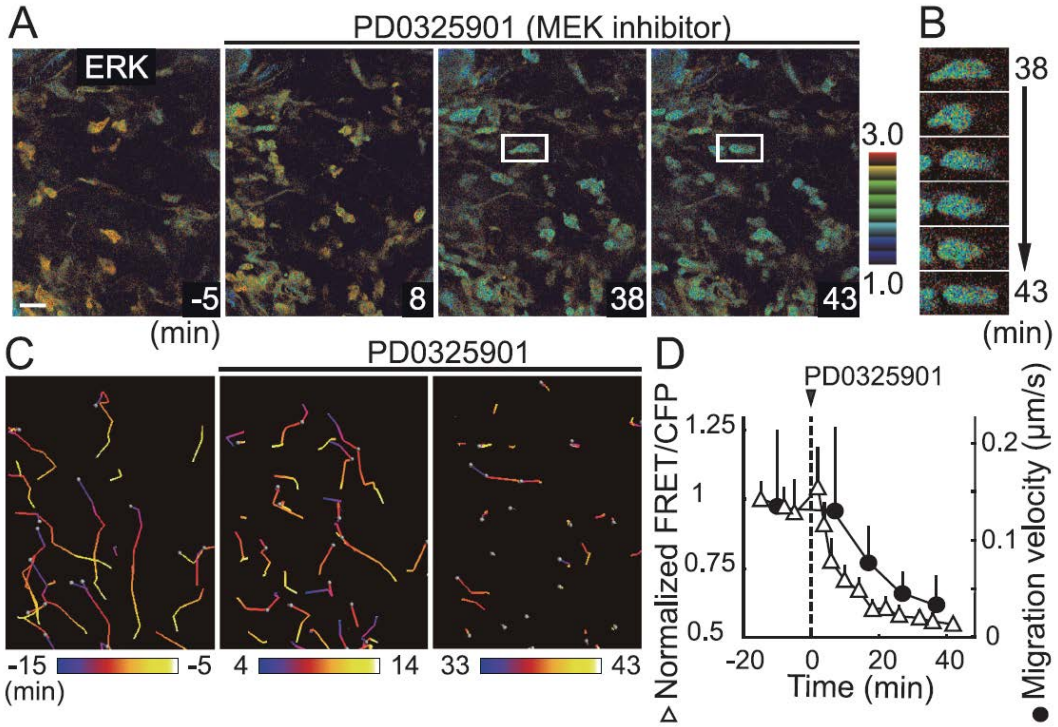

The activation of ERK in activated granulocytes prompted them to examine the effect of ERK inhibition on the migration of granulocytes induced by arachidonic acid.

- ERK activity in granulocytes dropped within a few minutes after i.v injection of a MEK inhibitor, PD0325901
- Granulocytes halted migration ~10 min after the inhibition of ERK activity.

Real-time visualization of pharmacodynamics in individual cells

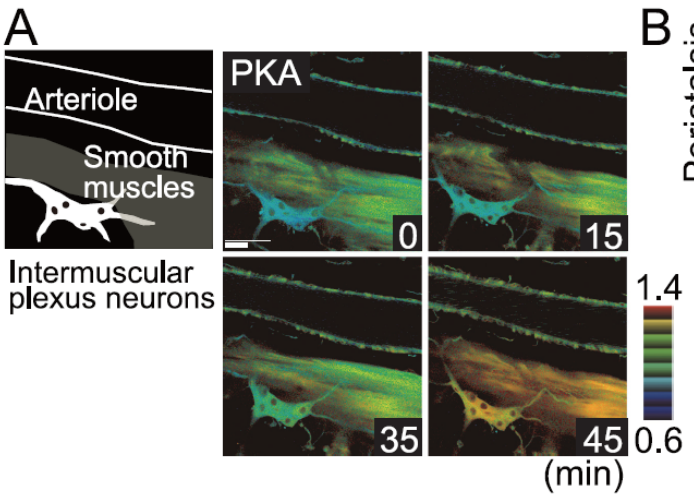

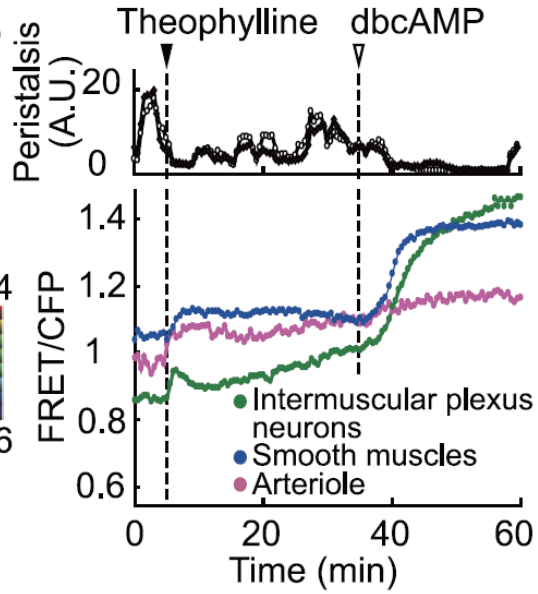

Theophylline and dbcAMP were i.v injected at 5 and 35 minutes.

Theophylline: a PKA activity phosphodiesterase inhibitor.

dbcAMP: a cAMP analogue, dibutyryl cyclic AMP.

Intestinal peristalsis was simultaneously quantified by the drift of the plexus neurons.

PKA activity was monitored in the muscular layer of the small intestine, where intermuscular plexus neurons, smooth muscles, and endothelial cells were observed for their sensitivity to Theophylline and dbcAMP.

- Upon theophylline administration, PKA activity increased modestly in the smooth muscle cells, endothelial cells, and intermuscular plexus neurons.
- Additional injection of dbcAMP fully activated PKA in the smooth muscle cells and intermuscular plexus neurons, which resulted in the cessation of peristalsis.

Real-time visualization of pharmacodynamics in individual cells

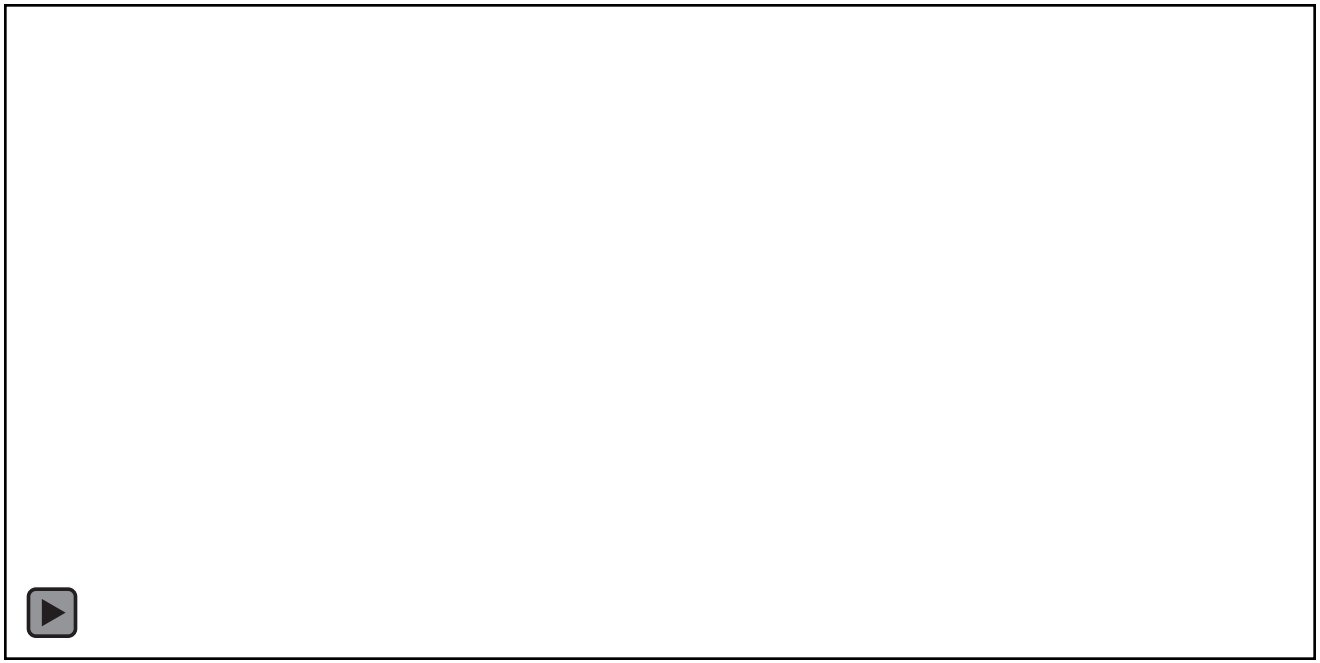

Theophylline and dbcAMP were i.v injected at 5 and 35 minutes

- The modest increase in PKA activated by theophylline was able to suppress the intestinal peristalsis only transiently.
- The injection of dbcAMP fully activated PKA in the smooth muscle cells and intermuscular plexus neurons, which resulted in the complete cessation of peristalsis.

Summary of paper-1

- This paper described the efficient generation of transgenic mouse lines expressing heritable and functional biosensors for ERK and PKA.
- These transgenic mice were created by the cytoplasmic co-injection of Tol2 transposase mRNA and a circular plasmid harbouring Tol2 recombination sites.
- Observation of these transgenic mice by two-photon excitation microscopy yielded real-time activity maps of ERK and PKA in various tissues, with greatly improved signal-to-background ratios.
- A promising application of these transgenic mice will be in monitoring of drug pharmacodynamics.

Paper-2

Oncogene (2015) **34,** 1051–1057

www.nature.com/onc

SHORT COMMUNICATION

Heterogeneity in ERK activity as visualized by *in vivo* FRET imaging of mammary tumor cells developed in MMTV-Neu mice

Y Kumagai[1], H Naoki[2], E Nakasyo[3], Y Kamioka[4,5], E Kiyokawa[6] and M Matsuda[1,4]

Human epidermal growth factor receptor2/Neu, which is overexpressed in about 30% of human breast cancers, transduces growth signals in large part via the Ras–Raf–MEK–ERK pathway. Nevertheless, it is a matter of controversy whether high ERK activity in breast cancer tissues correlates with better or worse prognosis, leaving the role of ERK activity in the progression of breast cancers unresolved. To address this issue, we live-imaged ERK activity in mammary tumors developed in mouse mammary tumor virus-Neu transgenic mice, which had been crossed with transgenic mice expressing a Förster resonance energy transfer biosensor for ERK.

Heterogeneity in ERK activity as visualized by in vivo FRET imaging

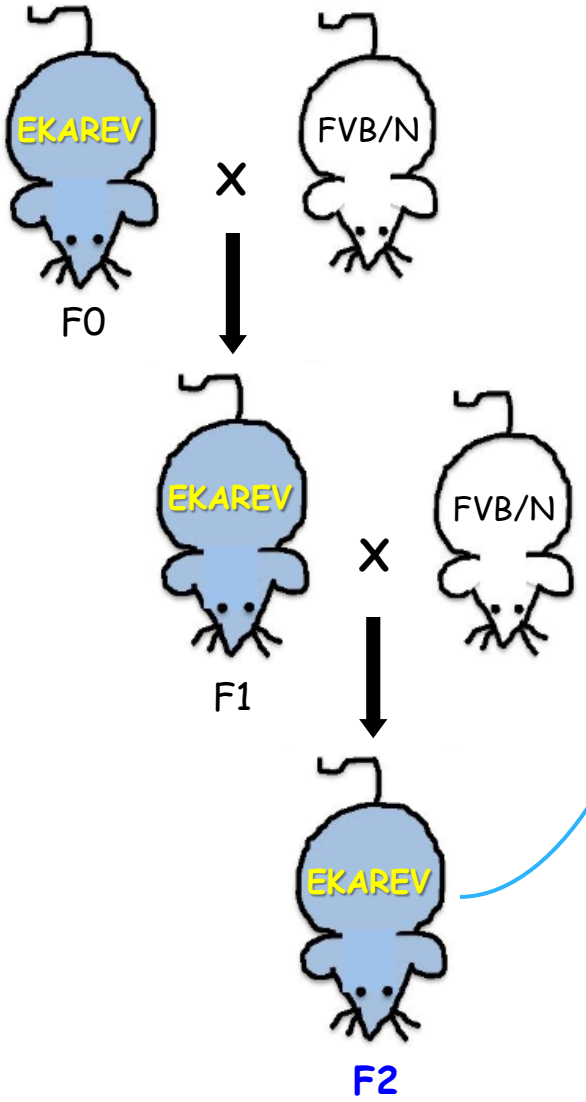

a widely used mouse model of HER2/Neu-positive luminal-type breast cancer

EKAREV$^{+/-}$ MMTV-Neu$^{+/+}$

developed mammary tumors from 24 weeks after birth

EKAREV$^{+/-}$/MMTV-Neu$^{+/-}$

indistinguishable from the parent MMTV-Neu$^{+/-}$ mice in size, the susceptibility to mammary tumor development, and the histological appearance of the developed tumors

Heterogeneity in ERK activity as visualized by in vivo FRET imaging

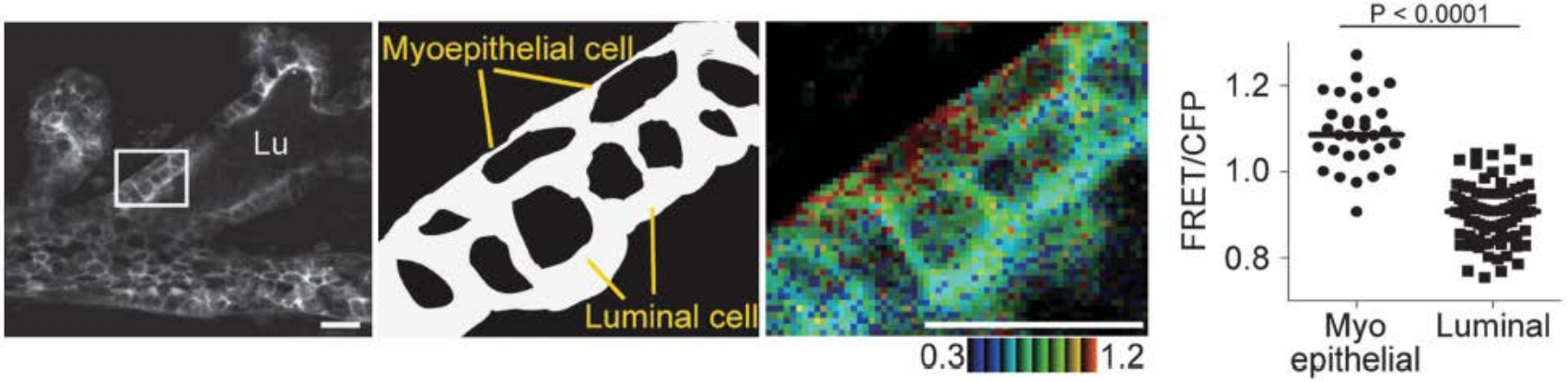

Observation of normal mammary glands of EKAREV$^{+/-}$ mice by two-photon microscopy (840 nm excitation wavelength)

- The ERK biosensor (EKAREV) was expressed both in luminal epithelial cells and myoepithelial cells.
- The level of ERK activity was higher in myoepithelial cells than luminal epithelial cells.

Heterogeneity in ERK activity as visualized by in vivo FRET imaging

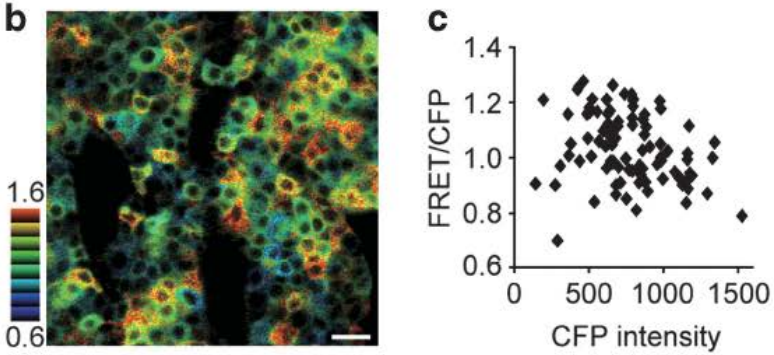

mammary tumors developed in EKAREV$^{+/-}$/MMTV-Neu$^{+/-}$ mice and observed under the 2P microscope

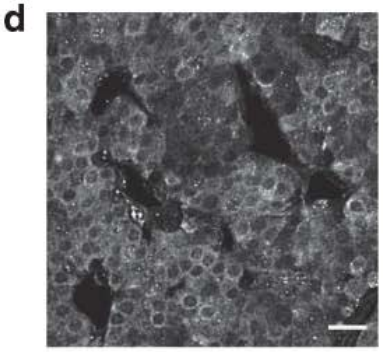

Immunostaining of a mammary tumor

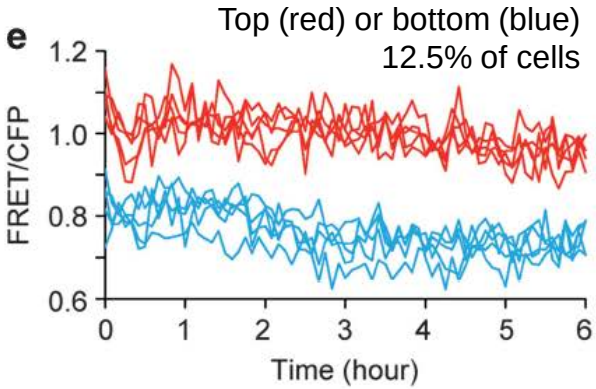

Mammary tumors were timelapse-imaged for 6 h to examine whether diversity in ERK activity was caused by temporal noise or population noise

- The tumor cells exhibited significant heterogeneity in ERK activity without forming any clusters with similar activity levels.
- No correlation between the FRET signal and the expression level of the biosensor suggested that the divergence in the FRET signal of mammary tumor cells reflected the heterogeneity in the ERK activity.
- The heterogeneity in the ERK activity by immunostaining with an anti-phospho-ERK antibody.
- The ERK activities relative to the average for the cell population did not change remarkably in most cells during the course of observation.

Real-time pharmacodynamics of anti-cancer drugs against ERK activity in the primary and secondary tumors

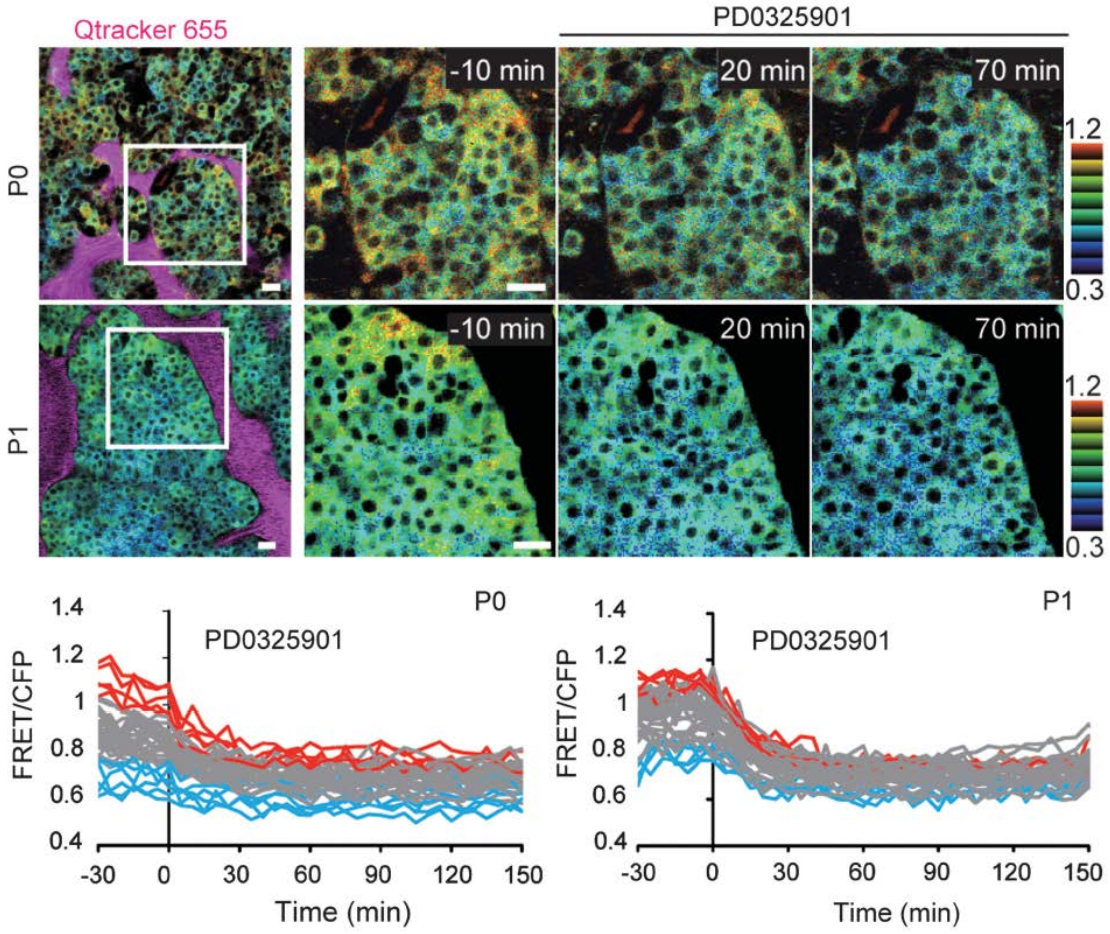

A MEK inhibitor under phase I trail (PD0325901) was i.v injected at time 0.

Qtracker 655 was i.v injected to visualize blood vessels.

The secondary tumors were appeared after the injection of the primary tumor into the mammary fat pad of syngeneic FVB mice.

- The MEK inhibitor immediately suppressed ERK activity in both the P0 and P1 mammary tumor cells with a half-time of ~ 10 min.

Real-time pharmacodynamics of anti-cancer drugs against ERK activity in the primary and secondary tumors

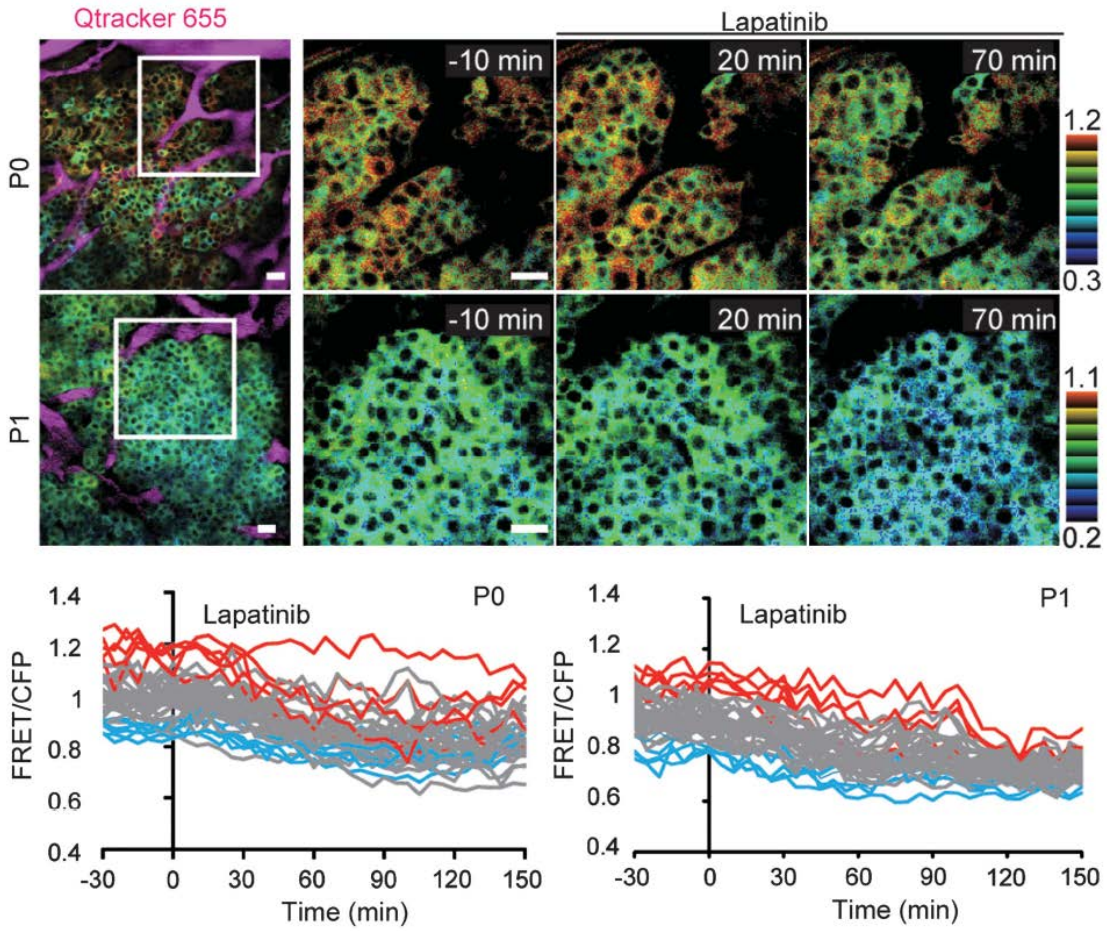

An EGFR/HER2 dual tyrosine kinase inhibitor, in clinical use (Lapatinib) was i.v injected at time 0.

Qtracker 655 was i.v injected to visualize blood vessels.

- Lapatinib gradually decreased the ERK activity from 10 min after injection in both the P0 and P1 mammary tumor cells.

Real-time pharmacodynamics of anti-cancer drugs against ERK activity in the primary and secondary tumors

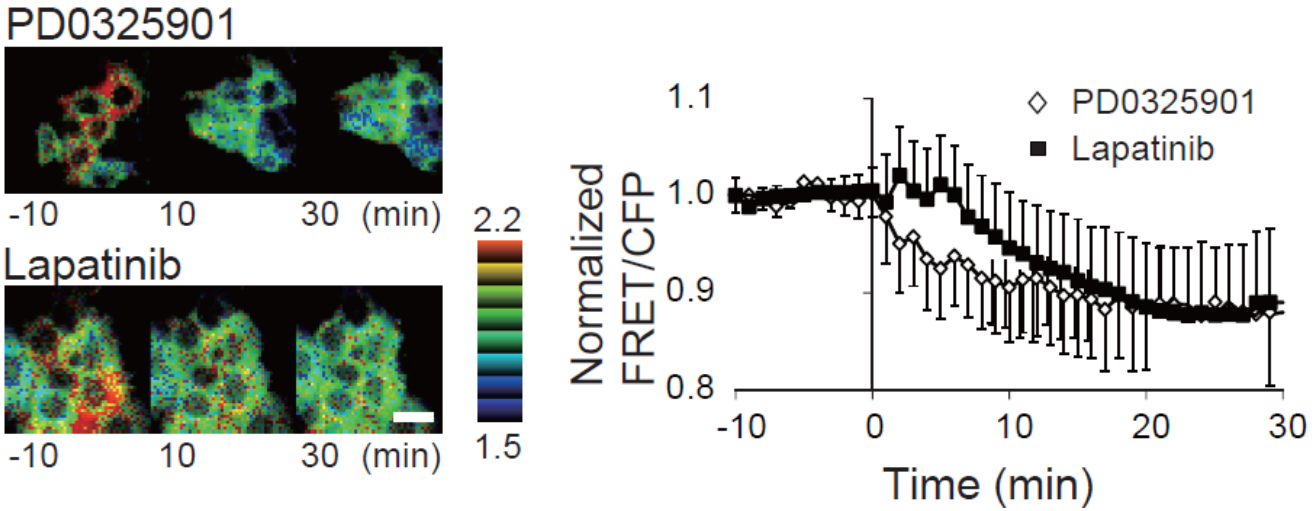

Response to inhibitors *in vitro*. Tumor cells plated on glass-base dishes. 1 μM PD0325901 or 10 μM Lapatinib, was added at time 0.

- The *in vitro* results also showed ERK activity in the Lapatinib treated cells started decreasing with ~ 5 min delay, suggesting that the delay was caused by the sensitivity of the tumor cells to Lapatinib.

Real-time pharmacodynamics of anti-cancer drugs against ERK activity in the primary and secondary tumors

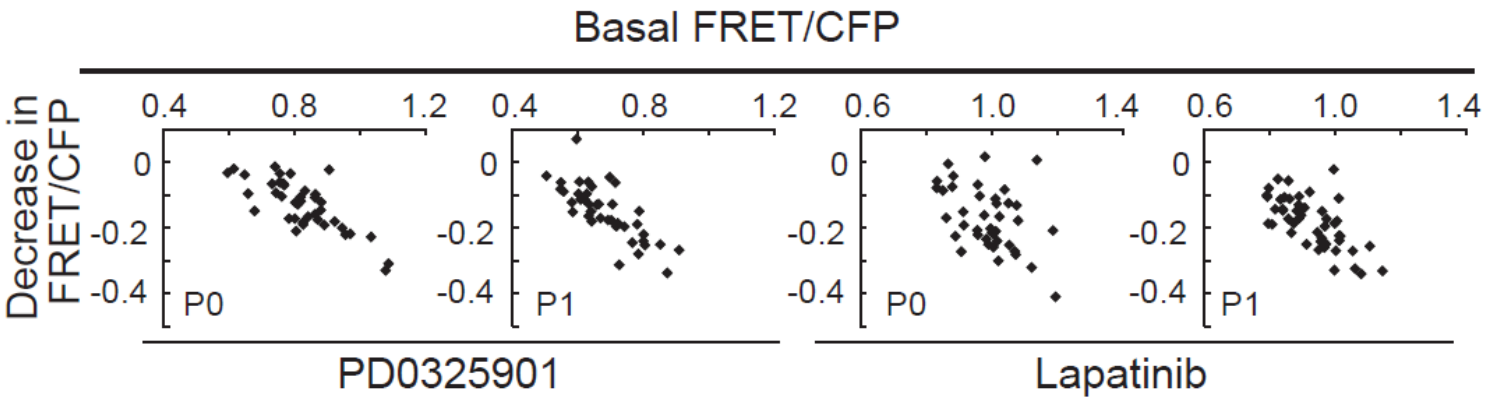

The decreases in FRET/CFP values 90 minutes after i.v injection of PD0325901 or Lapatinib are plotted against the FRET/CFP values before drug injection.

- The ERK activity decreased more significantly in high ERK-activity cells than in low ERK-activity cells.
- The low ERK-activity cells in the P0 tumors appeared to be the least-responsive cell population.

Real-time pharmacodynamics of anti-cancer drugs against ERK activity in the primary and secondary tumors

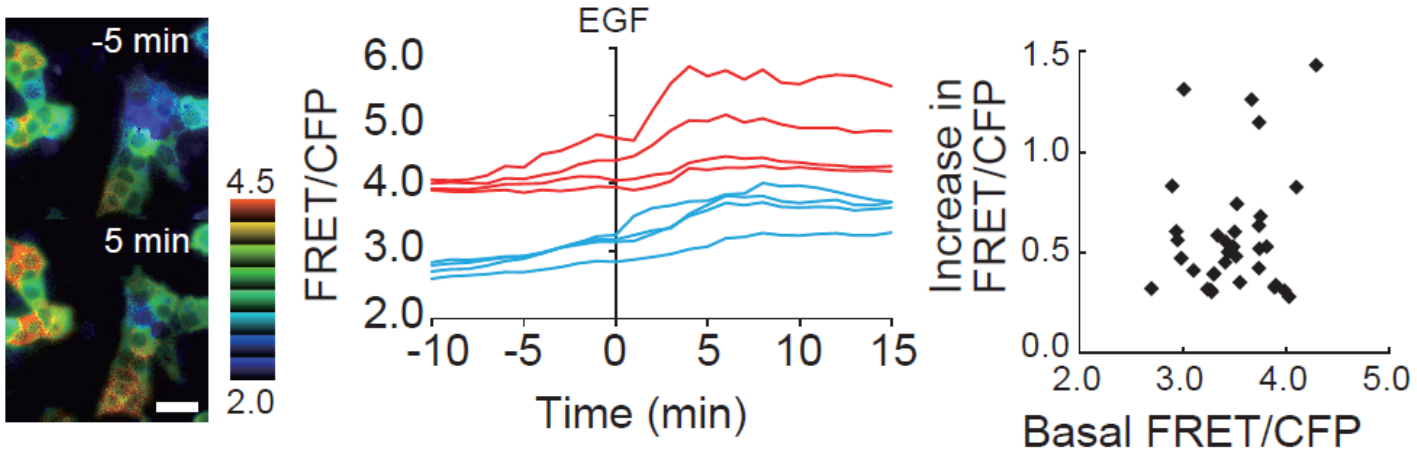

Response to EGF in vitro. EGF (10 ng/ml) was added at time zero.

- In contrast to the response to the inhibitors, no significant correlation was observed between the basal ERK activity and the EGF-induced increment.

Decreased tumorsphere formation efficiency and expression of CSC markers in tumor cells with high ERK activity

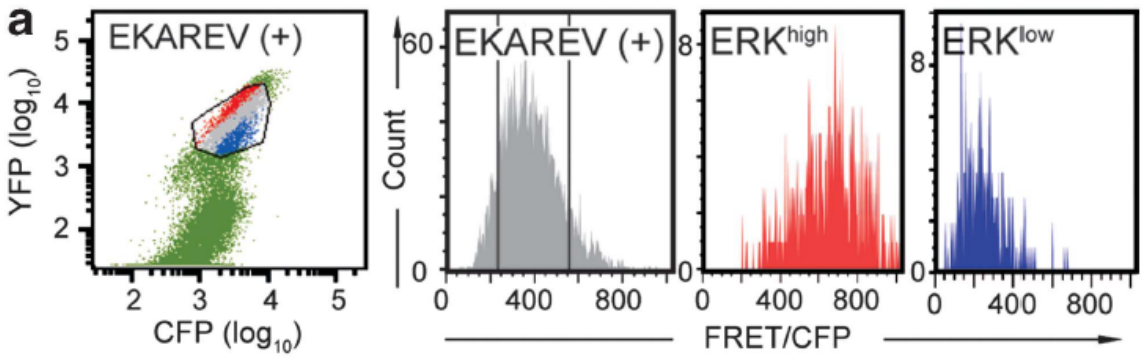

The mammary tumor tumor cells were sorted by FACS on the basis of their ERK activity.

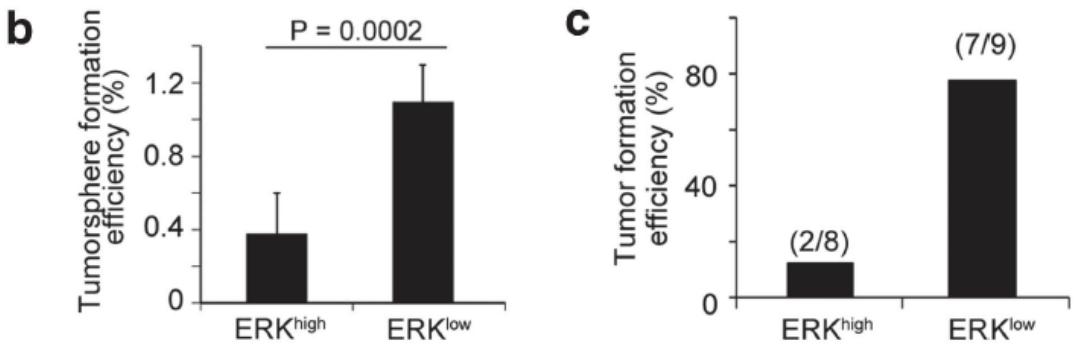

The ERK^{high} and ERK^{low} cells were plated in plates. Two weeks later, the tumorsphere formation was evaluated.

The ERK^{high} and ERK^{low} cells were injected into fat pads of syngeneic mice. Three months later, the development of tumors was assessed.

- By an *in vitro* tumorsphere formation assay, the ERK^{high} population exhibited lower tumorsphere formation efficiency compared with the ERK^{low} population.
- By an *in vivo* transplantation assay, the ERK^{high} population yielded tumors less efficiently than did the ERK^{low} population.

Decreased tumorsphere formation efficiency and expression of CSC markers in tumor cells with high ERK activity

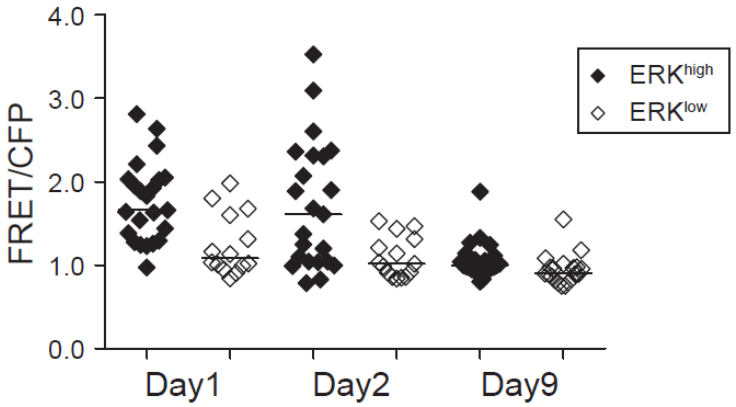

Cells were embedded in growth factor-reduced Matrigel (BD), cultured in DMEM/F12 medium and imaged with a laser scanning confocal microscope.

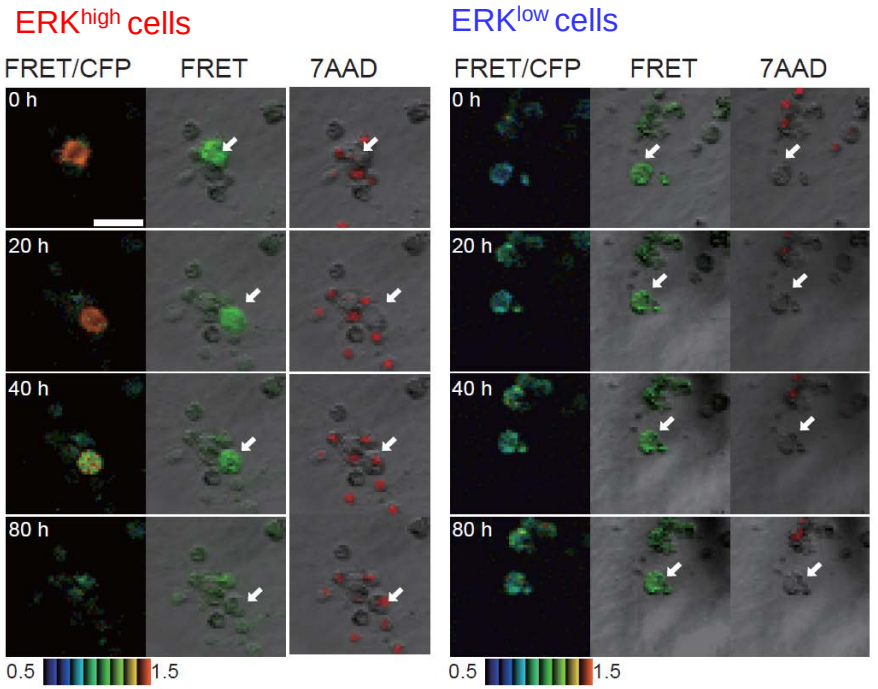

The fluorescent dyes (7AAD) accumulate in dead cells.

- The fraction of high ERK-activity cells in the ERK^{high} population decreased within 9 days to the level of those of the ERK^{low} population.
- The high ERK-activity cells died within 3 days, implying that the low tumorsphere formation efficiency of ERK^{high} cells is at least partially attributable to the vulnerability of ERK^{high} cell.

Suggested that high ERK activity may suppress the stemness of mammary tumor cells.

Decreased tumorsphere formation efficiency and expression of CSC markers in tumor cells with high ERK activity

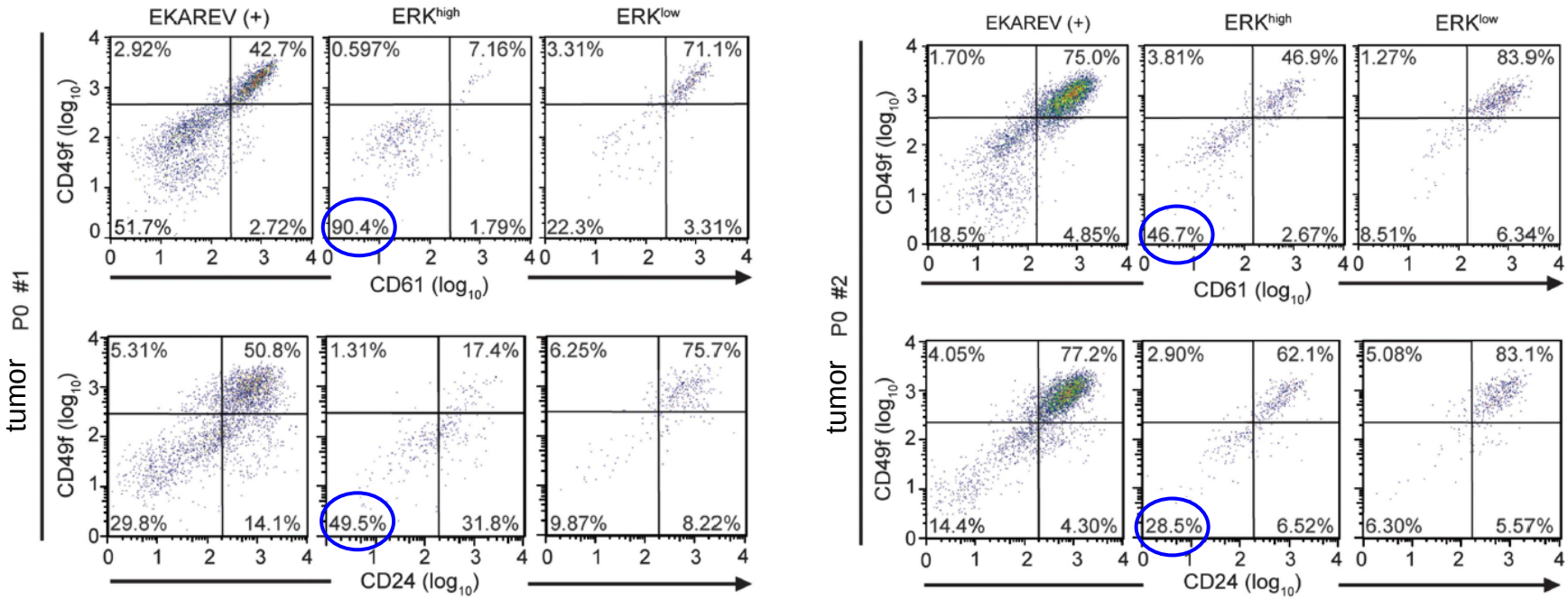

- A large portion of the MMTV-Neu tumor cells expressed three mammary stem cell markers, CD49f, CD24 and CD61.
- CD61−/CD49f− cells or CD24−/CD49f− cells were significantly increased in the ERK^{high} population.

Summary of paper-2

- Observation of the tumor by two-photon microscopy revealed significant heterogeneity in ERK activity among the mammary tumor cells.
- The level of ERK activity in each cell was stable up to several hours, implying a robust mechanism that maintained the ERK activity within a limited range.
- By sorting the mammary tumor cells on the basis of their ERK activity, they found that ERK^{high} cells less efficiently generated tumorspheres *in vitro* and tumors *in vivo* than did ERK^{low} cells.
- In agreement with this finding, the expressions of the cancer stem cell markers CD49f, CD24 and CD61 were decreased in ERK^{high} cells.
- These observations suggest that high ERK activity may suppress the self-renewal of mammary cancer stem cells, low ERK activity may be beneficial for self-renewal of the CSCs/TICs (cancer stem-like cells/tumor-initiating cells) of mammary tumor cells.

Advantages and challenges of FRET biosensors

Advantages

The ability to establish stable cell lines and transgenic mice expressing FRET biosensors provides a good tool to evaluate the effects of drugs on the pharmacodynamics and toxicity in living cells and animals.

- Reversible interactions can be measured.
- Distinct drug targets and redundant mechanisms can be measured simultaneously.
- The availability of intramolecular biosensors is steadily increasing.

Advantages and challenges of FRET biosensors

Challenges

- Both the distance and orientation of donor and acceptor affect the increase in FRET, but the 3D structure of the FRET biosensor cannot be predicted in most cases.
- The developers usually need to spend a rather lengthy period for the design, construction and evaluation, through multiple rounds of trial-and-error.
- Genetically engineered mouse models expressing FRET biosensors require careful selection of promotor or expression level for physiologically relevant tissue and lineage-specific expression.
- One of the limiting factors for these imaging modalities is the development of a 3D image processing program or algorithm.

More infomation: a detailed list of intramolecular single-chain FRET biosensors (1997-2015)
http://www.fret.lif.kyoto-u.ac.jp/e-phogemon/unifret2.htm

Future perspectives

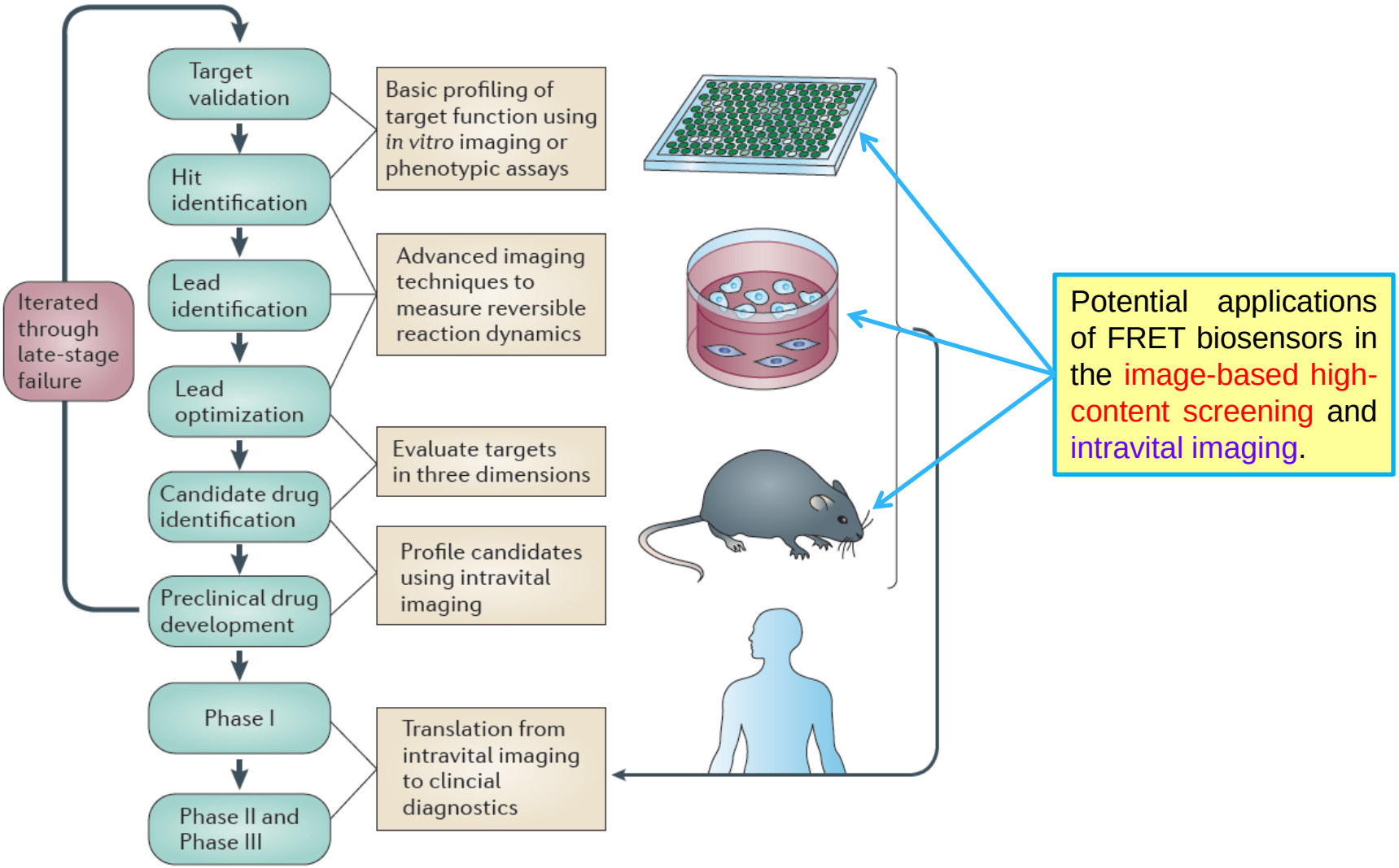

The core elements of the drug project operating model (DPOM)

Nat Rev Cancer. 2014 May;14(5):314-28.

Thank you for your attention !